Pten mediates Myc oncogene dependence in a conditional zebrafish model of T cell acute lymphoblastic leukemia

Alejandro Gutierrez,[1,3] Ruta Grebliunaite,[1] Hui Feng,[1] Elena Kozakewich,[1] Shizhen Zhu,[1] Feng Guo,[1] Elspeth Payne,[1] Marc Mansour,[1] Suzanne E. Dahlberg,[2] Donna S. Neuberg,[2] Jeroen den Hertog,[4] Edward V. Prochownik,[5] Joseph R. Testa,[6] Marian Harris,[7] John P. Kanki,[1] and A. Thomas Look[1,3]

[1]Department of Pediatric Oncology and [2]Department of Biostatistics and Computational Biology, Dana-Farber Cancer Institute, Boston, MA 02115
[3]Division of Hematology/Oncology, Children's Hospital Boston, Boston, MA 02115
[4]Hubrecht Institute, Utrecht 3584 CT, Netherlands
[5]Division of Hematology/Oncology, Children's Hospital of Pittsburgh, Pittsburgh, PA 15215
[6]Fox-Chase Cancer Center, Philadelphia, PA 19111
[7]Department of Pathology, Children's Hospital Boston, Boston, MA 02115

The MYC oncogenic transcription factor is overexpressed in most human cases of T cell acute lymphoblastic leukemia (T-ALL), often downstream of mutational *NOTCH1* activation. Genetic alterations in the PTEN–PI3K–AKT pathway are also common in T-ALL. We generated a conditional zebrafish model of T-ALL in which 4-hydroxytamoxifen (4HT) treatment induces MYC activation and disease, and withdrawal of 4HT results in T-ALL apoptosis and tumor regression. However, we found that loss-of-function mutations in zebrafish *pten* genes, or expression of a constitutively active *Akt2* transgene, rendered tumors independent of the MYC oncogene and promoted disease progression after 4HT withdrawal. Moreover, MYC suppresses *pten* mRNA levels, suggesting that Akt pathway activation downstream of MYC promotes tumor progression. Our findings indicate that Akt pathway activation is sufficient for tumor maintenance in this model, even after loss of survival signals driven by the MYC oncogene.

CORRESPONDENCE
Alejandro Gutierrez:
alejandro_gutierrez@dfci.harvard.edu
OR
A. Thomas Look:
thomas_look@dfci.harvard.edu

Abbreviations used: 4-hydroxytamoxifen, 4HT; T-ALL, T cell acute lymphoblastic leukemia.

The MYC oncogenic transcription factor is a key regulator of cell growth and proliferation that plays a central role in the pathogenesis of a wide range of human cancers (Pelengaris and Khan, 2003). In T cell acute lymphoblastic leukemia (T-ALL), *MYC* is typically overexpressed downstream of activated NOTCH1 (Palomero et al., 2006; Sharma et al., 2006; Weng et al., 2006). In most experimental models of MYC-induced tumorigenesis, ongoing MYC activity is required for tumor maintenance, and MYC down-regulation results in loss of the malignant phenotype via apoptosis or differentiation/senescence (Arvanitis and Felsher, 2006). Indeed, experimental evidence indicates that a subset of human T-ALL cell lines is dependent on aberrant *MYC* overexpression (Weng et al., 2006). Although Myc is required for normal cellular proliferation and development (Davis et al., 1993; Trumpp et al., 2001), recent work has demonstrated that the widespread inhibition of Myc, by expression of a dominant-interfering basic helix-loop-helix leucine zipper domain, is surprisingly well tolerated and induces regression of *Ras*-induced lung tumors (Soucek et al., 2008). These findings, together with advances in therapeutic targeting of protein–protein interactions, have rekindled interest in the development of clinically useful strategies for MYC inhibition (Verdine and Walensky, 2007; Prochownik and Vogt, 2010). Thus, elucidating the determinants of a tumor cell's response to MYC inhibition could have important therapeutic

The Rockefeller University Press $30.00
J. Exp. Med. Vol. 208 No. 8 1595-1603
www.jem.org/cgi/doi/10.1084/jem.20101691

consequences. Several tumor cell–intrinsic genetic determinants of *Myc* oncogene dependence have been identified, including *p16INK4a*, *Rb*, and *p53* (Wu et al., 2007), as well as an autocrine signaling pathway mediated by TGF-β (van Riggelen et al., 2010). Moreover, host-dependent mechanisms have also been implicated in tumor regression after Myc inactivation, involving inhibition of angiogenesis (Giuriato et al., 2006; Sodir et al., 2011) and the cellular immune system (Rakhra et al., 2010).

The PI3K–AKT signal transduction pathway, which is negatively regulated by the PTEN tumor suppressor, mediates oncogenic signaling downstream of growth factor receptors and is frequently dysregulated in human cancer (Chalhoub and Baker, 2009). We have recently identified genetic alterations within the PTEN–PI3K–AKT pathway in 48% of primary T-ALL patient samples (Gutierrez et al., 2009), clearly implicating this pathway in human T-ALL pathogenesis. Constitutive signaling though the PI3K–AKT pathway in T-ALL has been implicated in resistance to NOTCH1 inhibitors (Palomero et al., 2007), which are effective in part as a result of their downstream effect on *MYC* expression (Palomero et al., 2006; Sharma et al., 2006; Weng et al., 2006). In a mouse model of MYC-induced mammary tumorigenesis, loss of MYC dependence was strongly associated with the acquisition of activating mutations in *Kras2* (D'Cruz et al., 2001), suggesting that activation of signal transduction pathways downstream of RAS, such as the PI3K–AKT pathway, can overcome dependence on MYC. Moreover, MYC has recently been shown to promote signaling through the PI3K–AKT pathway via up-regulation of micro-RNAs that down-regulate *PTEN* (Mu et al., 2009; Olive et al., 2009; Kim et al., 2010; Mavrakis et al., 2010). Consistent with these findings, Myc inactivation was followed by transcriptional up-regulation of *Pten* in mouse Myc-dependent osteosarcomas (Wu et al., 2008). However, the hypothesis that the PTEN–PI3K–AKT pathway mediates Myc dependence has not previously been tested, as previous efforts to overexpress *Myc* in *Pten*-null mouse pancreatic β cells led to massive apoptosis without tumor development (Radziszewska et al., 2009).

In this manuscript, we used a conditional zebrafish model of *MYC*-induced T-ALL to test the hypothesis that AKT pathway activation can substitute for MYC signals required for tumor maintenance in vivo. We found that loss-of-function *pten* mutations or constitutive Akt activation were strongly associated with loss of MYC oncogene dependence, suggesting that PI3K–AKT pathway activation can functionally replace signals mediated by an activated MYC transgene in the maintenance of T-ALL transformation.

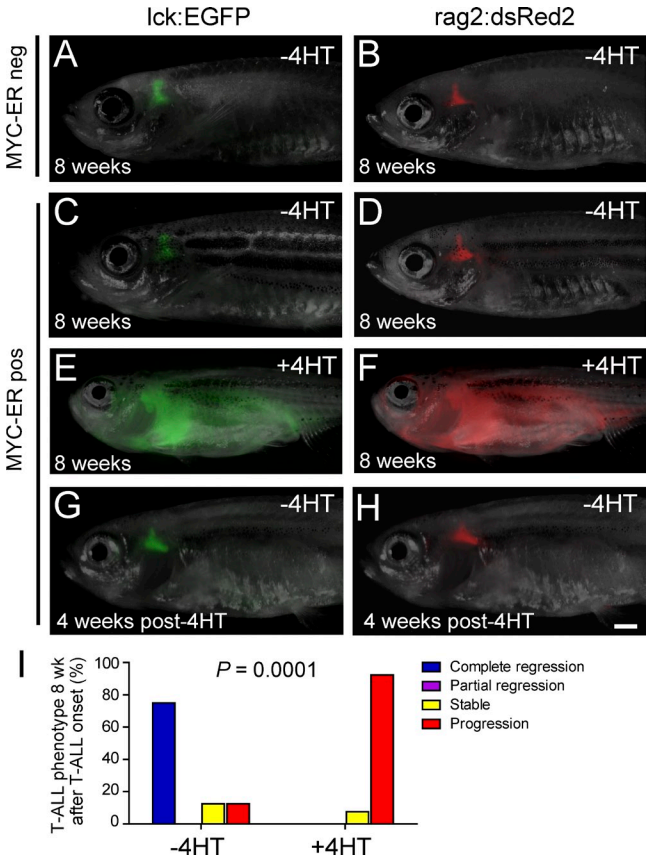

Figure 1. Conditional T-ALL development in *rag2:MYC-ER* transgenic zebrafish. (A and B) Thymic fluorescence in control MYC-ER–negative *lck-EGFP* transgenic (A) and *rag2:dsRed2* transgenic (B) zebrafish raised in the absence of 4HT. (C and D) Thymic fluorescence in the absence of 4HT treatment in *rag2:MYC-ER* transgenic zebrafish that also expressed *lck-EGFP* (C) or *rag2:dsRed2* (D). For A–D, one representative zebrafish is shown from a minimum of eight fish raised in each condition. (E and F) Fully penetrant T-ALL in *rag2:MYC-ER* transgenic zebrafish raised in 50 µg/liter (129 nM) 4HT. A representative triple-transgenic *rag2:MYC-ER; lck:EGFP; rag2:dsRed2* zebrafish is shown at the time of disseminated T-ALL development, imaged in both green and red fluorescent channels. (G and H) Thymic fluorescence in the *rag2:MYC-ER* transgenic zebrafish from E and F, shown 4 wk after 4HT removal. In all triple-transgenic zebrafish in which regression occurred (n = 6 of 8), T-ALL regression occurred simultaneously in both green and red fluorescent channels, with no evidence of residual EGFP-positive dsRed2-negative mature T cells, indicating that differentiation was not the primary mechanism of T-ALL regression. Bar, 1 mm. (I) After T-ALL development, zebrafish were either removed from 4HT to down-regulate the MYC transgene (−4HT) or kept in 4HT (+4HT), and tumor phenotype was assessed 8 wk after 4HT removal. Zebrafish that became moribund with leukemia before the 8-wk time point were euthanized and classified into the progression category. Number of fish analyzed per condition: −4HT, n = 8; +4HT, n = 13.

RESULTS

Conditional T-ALL development in *rag2:MYC-ER* transgenic zebrafish

We previously generated a zebrafish model of T-ALL, using *rag2* promoter-driven expression of a mouse *EGFP-Myc* fusion transgene to induce T-ALL which closely resembles the human disease pathologically and by gene expression (Langenau et al., 2003, 2005a). To generate a zebrafish model of T-ALL in which MYC activity could be modulated in established tumor cells, we generated stable transgenic zebrafish expressing *rag2:MYC-ER*, in which the zebrafish *rag2* promoter drives expression of a fusion transgene consisting of human *MYC* fused to the ligand-binding domain of a modified

estrogen receptor that is posttranslationally induced by 4-hydroxytamoxifen (4HT) treatment but not by endogenous estrogens (Littlewood et al., 1995). When treated with vehicle control (ethanol), *rag2:MYC-ER* heterozygous fish did not develop T-ALL over a 16-wk follow-up period. Thymic fluorescence in 8-wk-old *rag2:MYC-ER* transgenic fish co-expressing *lck:EGFP* and *rag2:dsRed2* transgenes that were treated with vehicle control was indistinguishable from that of their *rag2:MYC-ER* negative siblings (Fig. 1, A–D). However, when MYC-ER was induced by treatment with 50 µg/liter (129 nM) 4HT beginning at 5 d postfertilization, *rag2:MYC-ER* transgenic zebrafish developed fully penetrant T-ALL starting at 5 wk of age (Fig. 1, E and F). Histological analysis of T-ALL tumors induced by *rag2:MYC-ER* alone revealed that these tumors consisted of sheets of monomorphic lymphoblasts characterized by regular nuclear contours, scant cytoplasm, homogeneous chromatin, and inconspicuous nucleoli (Fig. S1), morphological features which closely resemble those of human T-ALL lymphoblasts. Note that no phenotypic differences were observed between these tumor cells and those arising in zebrafish of other genotypes studied throughout this manuscript (Fig. S1).

To test whether these tumors were dependent on ongoing MYC transgene activation, zebrafish with T-ALL were removed from 4HT to down-regulate MYC activity, and tumors were monitored weekly for 8 wk by fluorescence imaging. Tumor phenotypes were then classified into four categories based on the degree of change in tumor size by the end of the 8-wk monitoring period: (1) complete regression (disappearance of all abnormal extrathymic fluorescence), (2) partial regression (reduction in tumor diameter to less than half its original size), (3) stable disease (tumors that did not meet criteria for regression or progression), and (4) progression (increase in tumor diameter to more than twice its original size). After T-ALL development, removal from 4HT induced complete tumor regression in 75% of zebrafish examined, whereas tumor regression was not seen in any of the zebrafish kept in 4HT (Fig. 1 I; $P = 0.0001$).

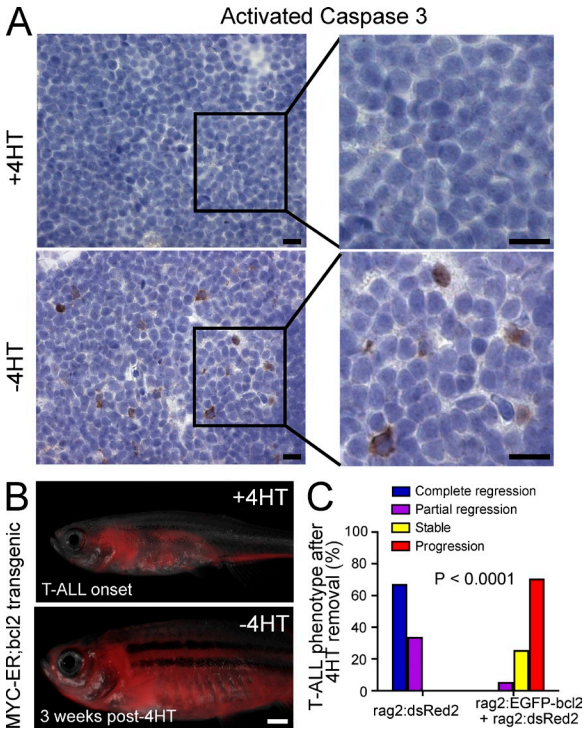

Figure 2. T-ALL regression after MYC down-regulation occurs via mitochondrial apoptosis. (A) Immunohistochemical staining for the apoptotic marker activated caspase 3 was performed in *rag2:MYC-ER* transgenic zebrafish with T-ALL in the presence of 4HT (+4HT) and 4 d after 4HT removal (−4HT). Number of fish analyzed = 4 per condition. Bars, 10 µm. (B) One representative *rag2:MYC-ER; rag2:EGFP-bcl2; rag2:dsRed2* triple-transgenic zebrafish is shown at the time of T-ALL onset and 3 wk after removal from 4HT. Bar, 1 mm. (C) Quantitation of T-ALL phenotypes 8 wk after MYC-ER inactivation, comparing *rag2:EGFP-bcl2* transgenic zebrafish versus *rag2:dsRed2* controls. Number of fish analyzed per condition: *rag2:MYC-ER;rag2:dsRed2*, $n = 12$; *rag2:MYC-ER; rag2:dsRed2; rag2:EGFP-bcl2*, $n = 20$.

MYC down-regulation induces mitochondrial apoptosis in T lymphoblasts

In most experimental models of MYC-induced tumorigenesis, inactivation of MYC leads to loss of the malignant phenotype as a result of apoptotic cell death or differentiation/senescence (Arvanitis and Felsher, 2006). To examine the fate of T-ALL cells in *rag2:MYC-ER* zebrafish after 4HT withdrawal, we monitored EGFP expression driven by the lck promoter, which is expressed in both immature and mature T cells, and dsRed2 expression driven by the rag2 promoter, which is expressed in immature but not mature T cells (Langenau et al., 2004, 2005a). The loss of tumor cells after removal from 4HT did not appear to predominantly represent T cell differentiation because in each fish with tumor regression we noted the simultaneous disappearance of disseminated cells expressing both EGFP and dsRed2 fluorescence, with no visible residual extrathymic EGFP-positive dsRed2-negative mature T cells (Fig. 1, E–H). Furthermore, examination of the senescence marker acidic β-galactosidase activity revealed no increase above background levels in T-ALL cells after MYC inactivation (Fig. S2). In some settings, collapse of the tumor-associated vasculature is involved in tumor regression after MYC inactivation (Giuriato et al., 2006; Sodir et al., 2011); thus, we also examined whether MYC inactivation affected the tumor vasculature, taking advantage of *fli1:EGFP* transgenic zebrafish in which EGFP is robustly expressed in vascular endothelium (Lawson and Weinstein, 2002). Immunohistochemistry for EGFP in *rag2:MYC-ER;rag2:dsRed2;fli1:EGFP* triple-transgenic zebrafish revealed no significant differences in tumor-associated microvascular density 4 d after MYC inactivation (Fig. S3).

Immunohistochemical analysis of T-ALL cells from *rag2:MYC-ER* transgenic zebrafish revealed increased staining for the apoptotic marker activated caspase 3 after removal from 4HT (Fig. 2 A), implicating the induction of apoptotic cell death in T-ALL cells after MYC down-regulation. We thus reasoned

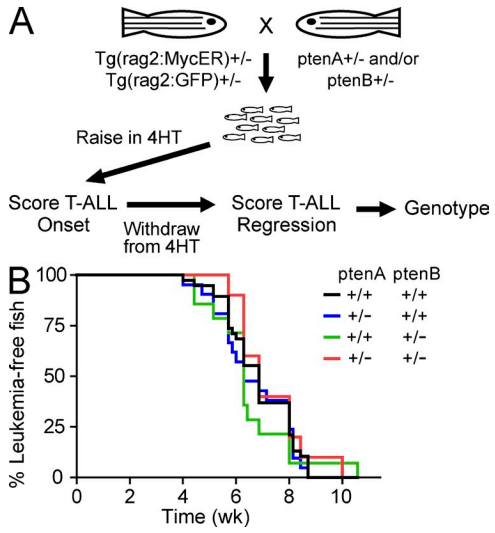

Figure 3. *pten* haploinsufficiency does not accelerate onset of MYC-induced T-ALL. (A) Experimental design to test the effect of *pten* haploinsufficiency on T-ALL onset upon MYC-ER activation and on tumor regression after 4HT removal. (B) Analysis of T-ALL onset in zebrafish from the experiment described in A. Number of fish analyzed per genotype: ptenA +/+, ptenB +/+, $n = 39$; ptenA +/−, ptenB +/+, $n = 22$; ptenA +/+, ptenB +/−, $n = 12$; ptenA +/−, ptenB +/−, $n = 10$.

that mitochondrial (intrinsic) apoptosis might be the key mediator of T-ALL regression after MYC down-regulation, a hypothesis which we tested using a *rag2:EGFP-bcl2* transgene, which blocks intrinsic apoptosis in thymocytes by binding and sequestering proapoptotic BCL2 family proteins (Langenau et al., 2005b). Indeed, we found that T-ALL tumors induced in *rag2:MYC-ER* zebrafish that also expressed *rag2:EGFP-bcl2* failed to regress after MYC down-regulation (Fig. 2, B and C; $P < 0.0001$). Collectively, these findings implicate mitochondrial apoptosis as a central mediator of T-ALL regression after MYC down-regulation in this model.

Pten inactivating mutations promote loss of MYC oncogene dependence

We have recently identified genetic alterations of *PTEN* and the *PI3K-AKT* pathway in 48% of primary T-ALL human tumor specimens, most of which (86%) were also characterized by *MYC* overexpression (Gutierrez et al., 2009). We thus wanted to use our model to test the hypothesis that such alterations would render T-ALLs independent of MYC oncogenic activity for tumor maintenance. Because of a partial genome duplication event during teleost evolution, zebrafish have duplicated *pten* genes, known as *ptenA and ptenB*, both of which are highly conserved with mammalian PTEN genes, demonstrate phosphatase activity toward phosphatidylinositol(3,4,5)triphosphate, and have redundant roles during zebrafish development (Faucherre et al., 2008). Complete deficiency of all zebrafish *pten* alleles leads to embryonic lethality, whereas compound haploinsufficiency is compatible with normal development. To test whether *pten* is a modulator of *MYC* oncogene dependence, double-transgenic *rag2:MYC-ER;rag2:GFP* zebrafish were mated to fish harboring loss-of-function mutations in their *ptenA* and/or *ptenB* genes (Fig. 3 A). Offspring from these matings were raised in 50 µg/liter (129 nM) 4HT beginning at 5 d postfertilization, the time at which thymic fluorescence is first visible in *rag2:GFP* transgenic fish, and T-ALL onset was monitored by weekly GFP fluorescence imaging beginning at 4 wk of age. After development of disseminated T-ALL, fish were removed from 4HT to down-regulate MYC activity, and tumor phenotypes after 4HT removal were assessed based on the degree of change in tumor size by the end of the 8-wk monitoring period, as described in the previous section.

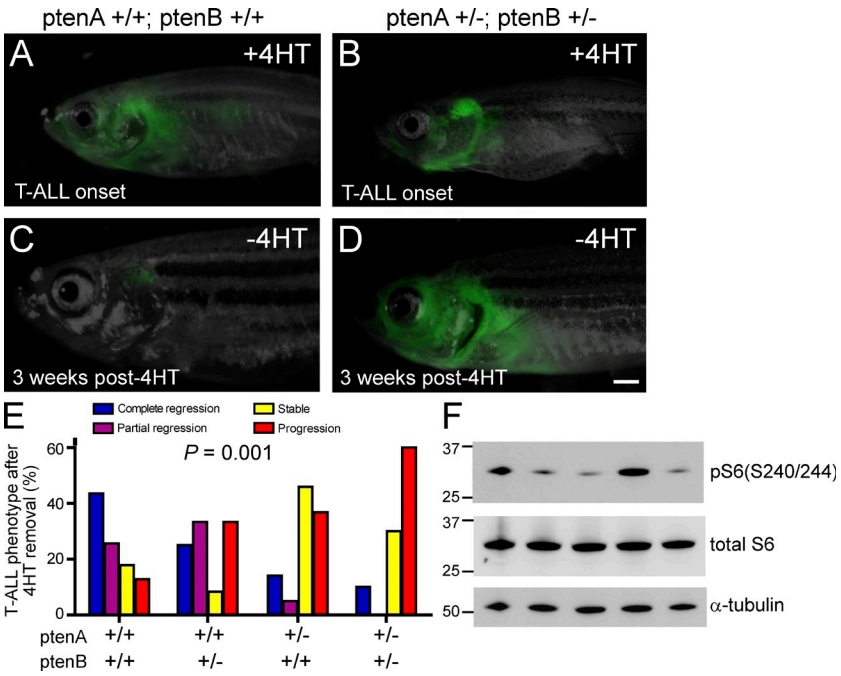

Figure 4. *pten* haploinsufficiency promotes loss of MYC transgene dependence. (A and C) One representative *rag2:MYC-ER; rag2:GFP* double-transgenic *pten*–wild-type zebrafish, shown at time of T-ALL onset (A) and 3 wk after removal from 4HT (C). (B and D) Representative *rag2:MYC-ER; rag2:GFP* double-transgenic zebrafish that harbored heterozygous mutations of both *ptenA* and *ptenB*, shown at time of T-ALL onset (B) and 3 wk after removal from 4HT (D). Bar, 1 mm. (E) Quantitation of T-ALL phenotypes after 4HT removal, based on *pten* genotype. Number of fish with T-ALL analyzed per genotype: *ptenA* +/+, *ptenB* +/+, $n = 39$; *ptenA* +/+, *ptenB* +/−, $n = 12$; *ptenA* +/−, *ptenB* +/+, $n = 22$; *ptenA* +/−, *pten*B +/−, $n = 10$. (F) Western blot analysis for phosphorylation of S6 ribosomal protein, a marker of Akt pathway activation, in sorted T-ALL cells from five different *rag2:MYC-ER* pten–wild-type zebrafish in which T-ALL progressed despite MYC down-regulation. Units for the molecular mass markers shown are in kD.

Loss of up to two of the four zebrafish *pten* alleles did not measurably accelerate the onset of MYC-induced T-ALL (Fig. 3 B); however, *pten* haploinsufficiency significantly promoted loss of tumor dependence on MYC transgene activation (Fig. 4). The rates of complete or partial regression were 69% in *pten* wild-type zebrafish, 58% in fish harboring heterozygous *ptenB* mutations, 18% in fish harboring heterozygous *ptenA* mutations, and 10% in *pten* double-heterozygous zebrafish (Fig. 4 E). Conversely, deficiency of *pten* also significantly promoted tumor progression after MYC-ER inhibition, with progression rates of 13% in *pten* wild-type zebrafish, 33 and 36% in fish harboring a single heterozygous mutation of *ptenB* or *ptenA*, respectively, and 60% in zebrafish harboring heterozygous mutations in both *ptenA* and *ptenB* (Fig. 4 E; $P = 0.001$ by 4×4 Fisher's exact test). Thus, *pten* haploinsufficiency strongly promoted the loss of *MYC* transgene dependence. Furthermore, Western blot analysis of the minority of T-ALL tumors from *rag2:MYC-ER pten*–wild-type zebrafish that progressed despite MYC down-regulation revealed that a subset of these tumors spontaneously acquired activation of the AKT pathway, as indicated by robust phosphorylation of S6 ribosomal protein (Fig. 4 F).

Constitutive Akt activation promotes loss of MYC oncogene dependence

Although PTEN is best known as a negative regulator of oncogenic signaling through the PI3K–AKT pathway, evidence also suggests that PTEN has AKT-independent functions, including regulation of p53 activity, chromosomal stability, and activity of the anaphase-promoting complex (Freeman et al., 2003; Shen et al., 2007; Song et al., 2011). To test whether *pten* deficiency modulates MYC dependence via Akt pathway activation, we tested whether expression of *rag2:myr-mAkt2*, encoding a myristoylated constitutively active mouse *Akt2* transgene (Tan et al., 2008), would phenocopy the effect of *pten* inactivation on MYC transgene dependence. Heterozygous *rag2:MYC-ER* zebrafish that did not harbor a thymic fluorescent transgene were out-crossed to wild-type animals, and all resultant embryos were injected at the one-cell stage with DNA expression constructs encoding *rag2:GFP* alone or both *rag2:GFP* and *rag2:myr-mAkt2*. Injected fish were raised in 4HT to induce T-ALL, after which 4HT was removed and tumor regression was monitored as in the previous section. Expression of *rag2:myr-mAkt2* significantly accelerated the onset of T-ALL in *rag2:MYC-ER* transgenic zebrafish, with a mean age at T-ALL onset of 4.3 wk in *rag2:myr-mAkt2*–injected fish, compared with 12.1 wk in control MYC-ER fish injected with *rag2:GFP* alone (Fig. 5 A; $P = 0.017$). Expression of *rag2:myr-mAkt2* in MYC-ER–negative zebrafish also induced T-ALL development in 17% of these fish by 20 wk (Fig. 5 A), indicating that Akt activation is sufficient to induce T-ALL in the zebrafish, albeit at a relatively low penetrance.

Analysis of T-ALL regression after 4HT removal demonstrated that expression of the constitutively active *myr-mAkt2* transgene was strongly associated with loss of MYC transgene dependence (Fig. 5, B and C), suggesting that the effect of *pten* inactivation is mediated by Akt. T-ALLs arising in *rag2:MYC-ER* transgenic zebrafish expressing both *rag2:myr-mAkt2* and *rag2:GFP* showing a complete or partial regression rate of 14% after MYC-ER inhibition, compared with a regression rate of 75% in *rag2:MYC-ER* controls injected with *rag2:GFP* alone. Concomitantly, tumor progression rates were 86% in *rag2:myr-mAkt2*–injected zebrafish, compared with 17% of *rag2:GFP*-injected controls (Fig. 5 D; $P = 0.0002$ by 2×4 Fisher's exact test).

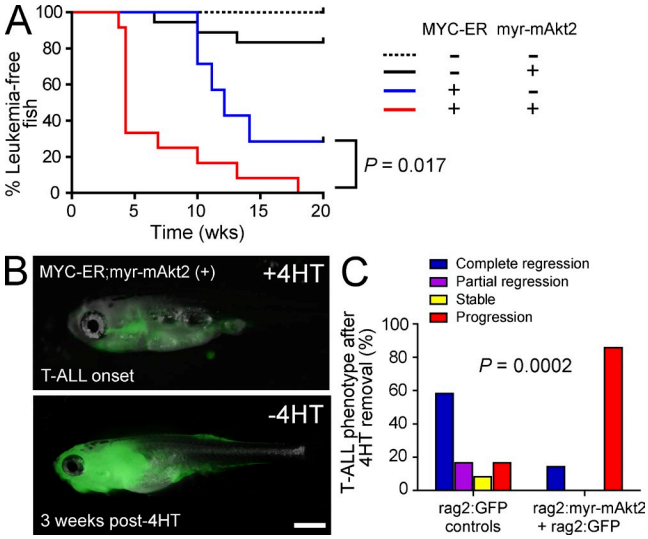

Figure 5. Constitutive Akt activation accelerates MYC-induced T-ALL and promotes loss of MYC transgene dependence. Germline *rag2:MYC-ER* heterozygous transgenic zebrafish were mated to wild-type fish, and all resultant offspring were injected at the one-cell stage with both *rag2:GFP* and *rag2:myr-mAkt2* (15 pg of each DNA construct) or with *rag2:GFP* alone (30 pg). (A) Kaplan-Meier analysis of leukemia-free survival based on genotype. Number of GFP-fluorescent fish analyzed per genotype: rag2:MYC-ER negative, rag2:myr-mAkt2 negative, $n = 10$; rag2:MYC-ER negative, rag2:myr-mAkt2 positive; $n = 18$. rag2:MYC-ER positive, rag2:myr-mAkt2 negative, $n = 12$; rag2:MYC-ER positive, rag2:myr-mAkt2 positive, $n = 21$. (B) Representative *rag2:MYC-ER* germline transgenic zebrafish injected with *rag2:myr-mAkt2* and *rag2:GFP*, shown at the time of T-ALL onset and 3 wk after removal from 4HT. Bar, 1 mm. (C) Quantitation of T-ALL phenotypes in *rag2:MYC-ER*–positive fish after 4HT removal, based on Akt genotype. Number of fish examined per group: rag2:myr-mAkt2, $n = 21$; rag2:GFP controls, $n = 12$.

Akt pathway activation does not alter the transcriptional activity of Myc

Activated Akt directly phosphorylates and inhibits GSK3 (Cross et al., 1995), which is a key regulator of Myc protein stability (Sears et al., 2000), thus we wanted to test whether Akt pathway activation might substitute for MYC transgene activation by inducing the transcriptional activity of endogenous Myc. The Ddx18 RNA helicase is a well established direct target of Myc in human and mouse cells (Grandori et al., 1996; O'Hagan et al., 2000), and we used injection of Myc mRNA into zebrafish embryos followed by ddx18 RNA in situ

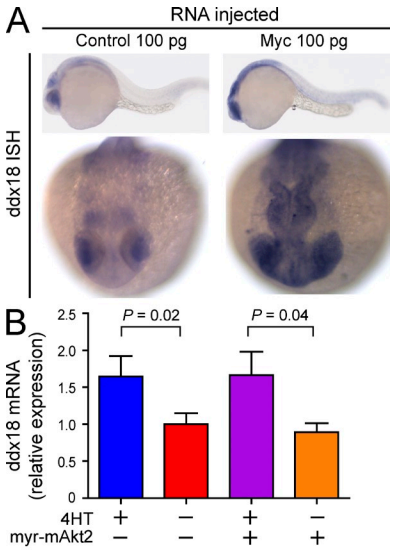

Figure 6. Expression of activated Akt does not alter the transcriptional activity of MYC. (A) Whole mount RNA in situ hybridization for *ddx18*, a known direct target of MYC in mammalian cells (Grandori et al., 1996; O'Hagan et al., 2000), performed at the 24-h postfertilization developmental stage in zebrafish embryos that were injected with 100 pg mCherry (control) or Myc mRNA at the one-cell stage. One representative zebrafish is shown in each condition out of a minimum of 20 embryos analyzed per condition. (B) Q-RT-PCR for *ddx18* expression, performed using RNA from T-ALL cells from *rag2:MYC-ER;rag2:EGFP-bcl2* zebrafish which also expressed either a *rag2:GFP* or a *rag2:myr-mAkt2* transgene. T-ALL cells were sorted from animals in 4HT (+4HT) or 4 d after 4HT removal (−4HT). β-Actin was used as the Q-RT-PCR control. Bcl2-transgenic T-ALL cells were used in all conditions to avoid comparing live versus dying cells after MYC-ER inactivation. Error bars represent standard error of the mean. Number of tumors analyzed per group: 4HT+, myr-mAkt2−, $n = 6$; 4HT−, myr-mAkt2−, $n = 7$; 4HT+, myr-mAkt2+, $n = 5$; 4HT−, myr-mAkt2+, $n = 5$.

hybridization to confirm that the regulation of *ddx18* by Myc is conserved in the zebrafish (Fig. 6 A). We then performed quantitative (Q) RT-PCR analysis of *ddx18* mRNA levels in sorted T-ALL cells from *rag2:MYC-ER;rag2:EGFP-bcl2* zebrafish that also expressed either a *rag2:GFP* or a *rag2:myr-mAkt2* transgene. T-ALL cells were sorted from zebrafish in 4HT and 4 d after 4HT removal. Expression of bcl2 was included in all conditions to avoid the confounding effects of apoptosis induction after MYC down-regulation in the absence of myr-mAkt2 expression. Analysis of the transcriptional activity of Myc, as assessed by *ddx18* Q-RT-PCR, revealed that it is regulated by 4HT treatment in *rag2:MYC-ER*–positive T-ALL cells, whereas the overexpression of constitutively active Akt had no effect on Myc transcriptional activity in the presence or absence of 4HT (Fig. 6 B). These findings were confirmed by Q-RT-PCR analysis for *npm1a*, a zebrafish orthologue of *NPM1*, another direct target of MYC (Zeller et al., 2001; Fig. S4). Collectively, these data indicate that the effect of Akt activation on Myc oncogene dependence is not mediated by increasing the transcriptional activity of endogenous Myc.

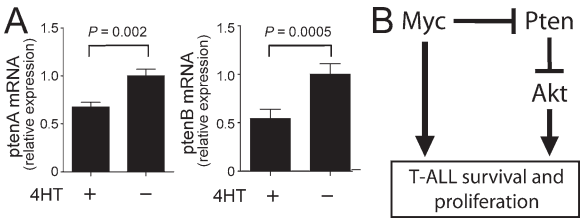

Figure 7. MYC represses *pten*. (A) Q-RT-PCR for *ptenA* and *ptenB* mRNA in T-ALL cells isolated from *rag2:MYC-ER; rag2:EGFP-bcl2* transgenic zebrafish before and 4 d after 4HT removal, demonstrated that both zebrafish *pten* transcripts are repressed by MYC. β-Actin was used as the Q-RT-PCR control. Error bars represent standard error of the mean. Number of tumors analyzed per condition: 4HT+, $n = 6$; 4HT−, $n = 7$−. (B) Model to explain our findings.

Myc represses Pten

The striking effect of *pten* haploinsufficiency on T-ALL regression after MYC down-regulation contrasted sharply with the absence of a detectable phenotype of *pten* haploinsufficiency on onset of MYC-induced T-ALL. We wondered whether T-ALLs arising in a *pten*-haploinsufficient background might have an increased propensity to loss of wild-type *pten* alleles, but sequencing of *ptenA* and *ptenB* cDNAs generated from T-ALL cells sorted at the time of tumor onset in *pten* wild-type and *pten* double-heterozygous fish ($n = 6$ tumors from each genotype) revealed no mutational inactivation of wild-type alleles in any of the tumors analyzed.

We reasoned that MYC-induced repression of *pten* might explain the lack of a phenotype induced by *pten* haploinsufficiency in the setting of high MYC activity, whereas a striking phenotype might be expected after MYC inactivation if this led to the relief of *pten* repression. We thus measured *ptenA* and *ptenB* mRNA levels by Q-RT-PCR in sorted T-ALL cells from *rag2:MYC-ER;rag2:EGFP-bcl2* transgenic zebrafish before and after 4HT removal. Q-RT-PCR analysis revealed that MYC down-regulation leads to a significant increase in transcript levels for both *ptenA* and *ptenB*, indicating that MYC represses *pten*, which is consistent with recent findings in mammalian cells (Mu et al., 2009; Olive et al., 2009; Kim et al., 2010; Mavrakis et al., 2010).

DISCUSSION

We have demonstrated for the first time that *pten* is an important mediator of MYC oncogene dependence in T-ALL lymphoblasts, an effect which appears to be mediated by its role as an inhibitor of oncogenic signaling through the Akt pathway. Furthermore, we also find that Myc represses Pten mRNA levels, an effect which is likely mediated by Myc-induced micro-RNAs which have recently been shown to down-regulate *Pten* (Mu et al., 2009; Olive et al., 2009; Kim et al., 2010; Mavrakis et al., 2010). Our data thus support a model in which Myc dependence is mediated in part by the up-regulation of Pten that follows Myc inactivation, which then acts to inhibit AKT pathway signaling which would otherwise be sufficient to maintain the malignant

phenotype, even in the absence of oncogenic signals mediated by Myc (Fig. 7 B).

Our findings implicate apoptotic cell death through the mitochondrial pathway as a critical mediator of Myc oncogene dependence in this model, thus indicating that inhibition of apoptosis downstream of AKT is the likely mechanism through which Pten haploinsufficiency induces loss of Myc oncogene dependence. Akt has previously been shown to inhibit mitochondrial apoptosis via multiple pathways (Manning and Cantley, 2007), including inactivation of BAD via phosphorylation (Datta et al., 1997; del Peso et al., 1997), transcriptional down-regulation of BIM downstream of its effect on FOXO proteins (Dijkers et al., 2002), inhibition of p53 via phosphorylation and activation of MDM2 (Mayo and Donner, 2001; Zhou et al., 2001), and up-regulation of the antiapoptotic MCL1 downstream of both mTOR (Wei et al., 2006; Hsieh et al., 2010) and GSK3 (Maurer et al., 2006). Our results indicate that AKT activation is one mechanism that can overcome MYC oncogene dependence in T-ALL, suggesting that PI3K-AKT inhibitors may have therapeutic utility in combination with inhibitors of MYC itself in the design of new therapeutic strategies for T-ALL.

MATERIALS AND METHODS

Transgenic and mutant zebrafish lines. The *rag2:MYC-ER* construct was generated by placing a human *MYC* transgene fused to the ligand-binding domain of the estrogen receptor, which is posttranslationally induced by 4HT but not endogenous estrogens (Littlewood et al., 1995), downstream of the zebrafish *rag2* promoter in a modified pBluescript vector in which the *rag2:MYC-ER* construct is flanked by recognition sequences for I-SceI meganuclease. This circular *rag2:MYC-ER* was co-injected together with a wild-type *mitfa* construct under its own promoter, also flanked by I-SceI recognition sequences, into one-cell stage embryos from the nacre line using a previously described I-SceI co-injection strategy (Grabher and Wittbrodt, 2008). Nacre zebrafish harbor a pigmentation defect caused by homozygous germline *mitfa* loss-of-function mutations, thus allowing rescue of the pigmentation defect by the co-injected *mitfa* transgene to act as a trans-genesis marker. A line derived from one *rag2:MYC-ER;mitf* founder zebrafish was identified that developed 4HT-dependent T-ALL and was used for all further studies. Co-segregation of the *rag2:MYC-ER* transgene together with the pigment-rescue phenotype was confirmed by PCR in all subsequent generations using the PCR primers described in the next section.

The *lck:EGFP*, *rag2:GFP*, *rag2:EGFP-bcl2*, and *fli1:EGFP* transgenic zebrafish lines have previously been described (Lawson and Weinstein, 2002; Langenau et al., 2003, 2004, 2005b). The transgenic line referred to here as *rag2:dsRed2* harbors a *rag2:LoxP-dsRed2-STOP-LoxP-EGFP-mMyc* transgene, which in the absence of Cre demonstrates dsRed2 expression driven by the rag2 promoter (Langenau et al., 2005a). It is worth noting that zebrafish expressing this construct demonstrate no detectable EGFP-Myc translation in the absence of Cre, as indicated by the absence of detectable EGFP fluorescence or spontaneous T-ALL development and by the lack of modification of T-ALL onset or regression in the *rag2:MYC-ER* line. Zebrafish harboring loss-of-function mutations in *ptenA* and *ptenB* genes were previously described (Faucherre et al., 2008).

The *rag2:myr-mAkt2* construct was generated by placing a myristoylated mouse Akt2 transgene (Tan et al., 2008), which is constitutively activated as a result of constitutive membrane localization, downstream of the rag2 promoter in the I-SceI–modified pBluescript vector described in the first paragraph in this section. Microinjections of the *rag2:myr-mAkt2* expression construct together with *rag2:GFP* (15 pg per embryo of each), or of *rag2:GFP* alone as a control (30 pg per embryo), were performed as previously described (Grabher and Wittbrodt, 2008). Zebrafish demonstrating thymic GFP fluorescence were examined for T-ALL development, and successful *rag2:myr-mAkt2* transgene integration was verified by PCR at the end of each experiment.

4HT treatment and T-ALL monitoring. Treatment with 4HT was begun starting at 5 d postfertilization, with each clutch placed in 750 ml of water containing 50 µg/liter (129 nM) 4HT (Sigma-Aldrich) in ethanol. Treatment with 4HT was performed offline, with weekly water changes beginning at 4 wk of age. Zebrafish raised in 4HT were screened for tumors by fluorescence microscopy weekly beginning at 4 wk of age. At the time of T-ALL onset and weekly during tumor regression monitoring, fish were imaged in both brightfield and GFP or dsRed2 fluorescent channels, as appropriate. Fluorescence microscopy was performed with a microscope (SMZ1500; Nikon) and an X-Cite 120 Fluorescence Illumination System (EXFO). Images were captured using a camera (DS2MBWc; Nikon) and NIS-Elements F Package (version 3.00; Nikon). All images shown represent merged fluorescence (shown in green or red, depending on the fluorophore) and brightfield (shown in grayscale) images. Fluorescence and brightfield images were merged using Photoshop (7.0; Adobe). Onset of T-ALL was defined as the development of a fluorescent mass arising from the thymus that was more than twice the size of normal thymus, together with invasion of adjacent tissues and structures. Note that we use T-ALL herein to refer to localized or disseminated T cell lymphoblastic tumors.

To monitor tumor regression, zebrafish with T-ALL were removed from 4HT and placed in individual tanks online, and tumors were imaged weekly for a total of 8 wk. Tumor phenotypes after 4HT removal were categorized into four classes based on the change in the diameter of the largest contiguous tumor mass by the end of the 8-wk monitoring period, as described in the Results section. Fish that became moribund with leukemia <8 wk after tamoxifen were euthanized and classified into the progression category. Genotyping for *rag2:MYC-ER*, as well as *ptenA* and *ptenB* or *rag2:myr-mAkt2*, was performed by genomic PCR after the completion of each experiment. PCR genotyping primers were as follows: *rag2:MYC-ER* forward, 5′-AGTCCTGAGACAGATCAGCA-3′, and reverse, 5′-TCATCATGCGGAACCGACTT-3′; and *rag2:myr-mAkt2* forward, 5′-ATGCTAATTTGAAGCACTAGCA-3′, and reverse, 5′-TTGGGTCCTTCTTCAGCAGT-3′. Genotyping for *ptenA* and *ptenB* was performed as previously described (Faucherre et al., 2008).

Zebrafish paraffin sectioning and immunohistochemistry. Zebrafish were euthanized in tricaine anesthetic, fixed in 4% paraformaldehyde at 4°C for 2 d, decalcified with 0.25 M EDTA, pH 8.0, for 2 d, dehydrated in alcohol, cleared in xylene, and embedded in paraffin. Slides were deparaffinized and pretreated with 10 mM citrate, pH 6.0, in a steam pressure cooker (Decloaking Chamber; BioCare Medical) according to the manufacturer's instructions, followed by washing in distilled water. Slides were pretreated with Peroxidase Block (Dako) for 5 min, followed by serum-free protein block (Dako) for 20 min to block nonspecific binding sites. Slides were then incubated with primary rabbit anticleaved caspase-3 antibody (1:50; Cell Signaling Technology) or mouse anti-GFP antibody (1:1500; Takara Bio Inc.). Secondary detection was performed by adding horseradish peroxidase-labeled polymer (Dako) for 30 min. Immunoperoxidase staining was developed with diaminobenzidine + chromogen kit (Dako), according to the manufacturer's instructions.

Zebrafish cryosectioning and β-galactosidase staining. Zebrafish were euthanized in tricaine anesthetic, embedded in a 1:1 mixture of 30% sucrose and Tissue-Tek O.C.T. compound (Sakura), and snap-frozen in isobutane precooled in dry ice. 14-µm frozen sections were cut onto slides using a CM3050 cryostat (Leica). Staining for activity of senescence-associated β-galactosidase was performed using the Senescence β-Galactosidase Staining kit (Cell Signaling Technology) according to the manufacturer's instructions.

Western blotting. DsRed2-sorted T-ALL cells were lysed in RIPA buffer (Millipore) supplemented with Complete Mini protease inhibitor (1 tablet/10 ml; Roche) and PhosSTOP phosphatase inhibitor (1 tablet/10 ml; Roche). 20 µg protein lysate was mixed with Laemmli 4× SDS sample buffer (Boston Bioproducts) and β-mercaptoethanol (Sigma-Aldrich) in appropriate

proportions and incubated at 100°C for 3 min before being run on a 4–12% Novex bis-tris polyacrylamide gel (Invitrogen) at 160V for 1 h. Blots were then transferred to a nitrocellulose membrane (Millipore) at 350 mA for 1 h, blocked with 5% milk in tris-buffered saline with 0.1% tween, and probed with anti–phospho-S6 ribosomal protein (Ser240/244) antibody (1:1,000; Cell Signaling Technology), anti-S6 ribosomal protein antibody (1:1,000; Cell Signaling Technology), and anti–α-tubulin antibody (1:1000; Cell Signaling Technology). Secondary detection was with HRP-linked antibodies (Cell Signaling Technology), HRP substrate was SuperSignal West Dura (Thermo Fisher Scientific), and Western blot images were captured using an ImageQuant LAS4000 chemiluminescent image analyzer (GE Healthcare).

RNA extraction and Q-RT-PCR. Total RNA was extracted from fluorophore-sorted T-ALL cells using Trizol reagent according to the manufacturer's instructions (Invitrogen). cDNA was synthesized from total RNA using the SuperScript III First-Strand Synthesis System for RT-PCR according to the manufacturer's instructions (Invitrogen). 3% of the cDNA reaction volume was then taken for each Q-RT-PCR reaction, performed with the SYBR green PCR Core Reagents kit (Applied Biosystems) and a 7300 Real Time PCR System instrument (Applied Biosystems) according to the manufacturer's instructions. All Q-RT-PCR were performed in triplicate, and *β-actin1* was used as the control for all Q-RT-PCR reactions. Q-RT-PCR primer sequences were as follows: *ddx18* forward, 5′-CGGCTGAGGAGGATAGTGATG-3′, and reverse, 5′-ACGCACCTGTCAGACCAGAAG-3′; *npm1a* forward, 5′-ACAAAAGGGCAAGAAGGAACAG-3′, and reverse, 5′-CGGCTAAAGTCCGTGGTGTTT-3′; *ptenA* forward, 5′-ATCCCCAGGGCTTCAAGAA-3′, and reverse, 5′-TGTGGATCTTTACCTTCAACTGATACA-3′; *ptenB* forward, 5′-GGGTGTCATGATTTGTGCGTACT-3′, and reverse, 5′-TCGCCTCTGACTGGGAATAGTC-3′; *β-actin1* forward, 5′-TACAATGAGCTCCGTGTTGC-3′, and reverse, 5′-ACATACATGGCAGGGGTGTT-3′.

Myc RNA injection into zebrafish embryos and ddx18 in situ hybridization. Mouse *Myc* was cloned into the pCS2$^+$ vector and linearized by Not1 digestion. *Myc* mRNA was then transcribed in vitro using the Ambion SP6 mMessage mMachine kit (Applied Biosystems). Zebrafish embryos were injected at the one-cell stage with 100 pg of *Myc* or control mCherry mRNA. At the 24-h postfertilization developmental stage, injected embryos were fixed overnight in 4% paraformaldehyde, and *ddx18* RNA in situ hybridization was performed as previously described (Payne et al., 2011).

Statistical analyses. Differences in tumor-free survival were assessed by the log-rank test, and time-to-event distributions were estimated via the Kaplan-Meier method. Differences in categorical data were assessed via Fisher's exact test, and differences in continuous data were assessed via the Mann-Whitney (rank-sum) test.

Online supplemental material. Fig. S1 shows histological morphology of T-ALL lymphoblasts of various genotypes analyzed in this study. Fig. S2 shows analysis of the senescence marker acidic β-galactosidase activity in sectioned *rag2:MYC-ER; rag2:dsRed2* double-transgenic zebrafish with T-ALL before and after 4HT withdrawal. Fig. S3 shows analysis of microvascular density in T-ALL tumors before and after 4HT withdrawal. Fig. S4 shows the effect of 4HT treatment versus withdrawal, and of expression of activated Akt2 versus control, on mRNA expression of the Myc target *npm1a*. Online supplemental material is available at http://www.jem.org/cgi/content/full/jem.20101691/DC1.

We thank Greg Molind and Lu Zhang for zebrafish husbandry.

This work was supported by National Institutes of Health grants NCI 5P01CA68484 and NCI 1K08CA133103 and by the William Lawrence Foundation. A. Gutierrez is a Scholar of the American Society of Hematology-Harold Amos Medical Faculty Development Program. H. Feng is supported by an award from the National Cancer Institute (NCI)/National Institutes of Health (K99CA134743). This work was also supported in part by grant P30 CA-06927 from the National Cancer Institute and by an appropriation from the Commonwealth of Pennsylvania.

The authors have no competing financial interests.

Submitted: 13 August 2010
Accepted: 9 June 2011

REFERENCES

Arvanitis, C., and D.W. Felsher. 2006. Conditional transgenic models define how MYC initiates and maintains tumorigenesis. *Semin. Cancer Biol.* 16:313–317. doi:10.1016/j.semcancer.2006.07.012

Chalhoub, N., and S.J. Baker. 2009. PTEN and the PI3-kinase pathway in cancer. *Annu. Rev. Pathol.* 4:127–150. doi:10.1146/annurev.pathol.4.110807.092311

Cross, D.A., D.R. Alessi, P. Cohen, M. Andjelkovich, and B.A. Hemmings. 1995. Inhibition of glycogen synthase kinase-3 by insulin mediated by protein kinase B. *Nature*. 378:785–789. doi:10.1038/378785a0

D'Cruz, C.M., E.J. Gunther, R.B. Boxer, J.L. Hartman, L. Sintasath, S.E. Moody, J.D. Cox, S.I. Ha, G.K. Belka, A. Golant, et al. 2001. c-MYC induces mammary tumorigenesis by means of a preferred pathway involving spontaneous Kras2 mutations. *Nat. Med.* 7:235–239. doi:10.1038/84691

Datta, S.R., H. Dudek, X. Tao, S. Masters, H. Fu, Y. Gotoh, and M.E. Greenberg. 1997. Akt phosphorylation of BAD couples survival signals to the cell-intrinsic death machinery. *Cell*. 91:231–241. doi:10.1016/S0092-8674(00)80405-5

Davis, A.C., M. Wims, G.D. Spotts, S.R. Hann, and A. Bradley. 1993. A null c-myc mutation causes lethality before 10.5 days of gestation in homozygotes and reduced fertility in heterozygous female mice. *Genes Dev.* 7:671–682. doi:10.1101/gad.7.4.671

del Peso, L., M. González-García, C. Page, R. Herrera, and G. Nuñez. 1997. Interleukin-3-induced phosphorylation of BAD through the protein kinase Akt. *Science*. 278:687–689. doi:10.1126/science.278.5338.687

Dijkers, P.F., K.U. Birkenkamp, E.W. Lam, N.S. Thomas, J.W. Lammers, L. Koenderman, and P.J. Coffer. 2002. FKHR-L1 can act as a critical effector of cell death induced by cytokine withdrawal: protein kinase B–enhanced cell survival through maintenance of mitochondrial integrity. *J. Cell Biol.* 156:531–542. doi:10.1083/jcb.200108084

Faucherre, A., G.S. Taylor, J. Overvoorde, J.E. Dixon, and J. Hertog. 2008. Zebrafish pten genes have overlapping and non-redundant functions in tumorigenesis and embryonic development. *Oncogene*. 27:1079–1086. doi:10.1038/sj.onc.1210730

Freeman, D.J., A.G. Li, G. Wei, H.H. Li, N. Kertesz, R. Lesche, A.D. Whale, H. Martinez-Diaz, N. Rozengurt, R.D. Cardiff, et al. 2003. PTEN tumor suppressor regulates p53 protein levels and activity through phosphatase-dependent and -independent mechanisms. *Cancer Cell*. 3:117–130. doi:10.1016/S1535-6108(03)00021-7

Giuriato, S., S. Ryeom, A.C. Fan, P. Bachireddy, R.C. Lynch, M.J. Rioth, J. van Riggelen, A.M. Kopelman, E. Passegué, F. Tang, et al. 2006. Sustained regression of tumors upon MYC inactivation requires p53 or thrombospondin-1 to reverse the angiogenic switch. *Proc. Natl. Acad. Sci. USA*. 103:16266–16271. doi:10.1073/pnas.0608017103

Grabher, C., and J. Wittbrodt. 2008. Recent advances in meganuclease-and transposon-mediated transgenesis of medaka and zebrafish. *Methods Mol. Biol.* 461:521–539. doi:10.1007/978-1-60327-483-8_36

Grandori, C., J. Mac, F. Siëbelt, D.E. Ayer, and R.N. Eisenman. 1996. Myc-Max heterodimers activate a DEAD box gene and interact with multiple E box-related sites in vivo. *EMBO J.* 15:4344–4357.

Gutierrez, A., T. Sanda, R. Grebliunaite, A. Carracedo, L. Salmena, Y. Ahn, S. Dahlberg, D. Neuberg, L.A. Moreau, S.S. Winter, et al. 2009. High frequency of PTEN, PI3K, and AKT abnormalities in T-cell acute lymphoblastic leukemia. *Blood*. 114:647–650. doi:10.1182/blood-2009-02-206722

Hsieh, A.C., M. Costa, O. Zollo, C. Davis, M.E. Feldman, J.R. Testa, O. Meyuhas, K.M. Shokat, and D. Ruggero. 2010. Genetic dissection of the oncogenic mTOR pathway reveals druggable addiction to translational control via 4EBP-eIF4E. *Cancer Cell*. 17:249–261. doi:10.1016/j.ccr.2010.01.021

Kim, J.W., S. Mori, and J.R. Nevins. 2010. Myc-induced microRNAs integrate Myc-mediated cell proliferation and cell fate. *Cancer Res.* 70:4820–4828. doi:10.1158/0008-5472.CAN-10-0659

Langenau, D.M., D. Traver, A.A. Ferrando, J.L. Kutok, J.C. Aster, J.P. Kanki, S. Lin, E. Prochownik, N.S. Trede, L.I. Zon, and A.T. Look. 2003. Myc-induced T cell leukemia in transgenic zebrafish. *Science*. 299:887–890. doi:10.1126/science.1080280

Langenau, D.M., A.A. Ferrando, D. Traver, J.L. Kutok, J.P. Hezel, J.P. Kanki, L.I. Zon, A.T. Look, and N.S. Trede. 2004. In vivo tracking of T cell development, ablation, and engraftment in transgenic zebrafish. *Proc. Natl. Acad. Sci. USA*. 101:7369–7374. doi:10.1073/pnas.0402248101

Langenau, D.M., H. Feng, S. Berghmans, J.P. Kanki, J.L. Kutok, and A.T. Look. 2005a. Cre/lox-regulated transgenic zebrafish model with conditional myc-induced T cell acute lymphoblastic leukemia. *Proc. Natl. Acad. Sci. USA*. 102:6068–6073. doi:10.1073/pnas.0408708102

Langenau, D.M., C. Jette, S. Berghmans, T. Palomero, J.P. Kanki, J.L. Kutok, and A.T. Look. 2005b. Suppression of apoptosis by bcl-2 overexpression in lymphoid cells of transgenic zebrafish. *Blood*. 105:3278–3285. doi:10.1182/blood-2004-08-3073

Lawson, N.D., and B.M. Weinstein. 2002. In vivo imaging of embryonic vascular development using transgenic zebrafish. *Dev. Biol.* 248:307–318. doi:10.1006/dbio.2002.0711

Littlewood, T.D., D.C. Hancock, P.S. Danielian, M.G. Parker, and G.I. Evan. 1995. A modified oestrogen receptor ligand-binding domain as an improved switch for the regulation of heterologous proteins. *Nucleic Acids Res.* 23:1686–1690. doi:10.1093/nar/23.10.1686

Manning, B.D., and L.C. Cantley. 2007. AKT/PKB signaling: navigating downstream. *Cell*. 129:1261–1274. doi:10.1016/j.cell.2007.06.009

Maurer, U., C. Charvet, A.S. Wagman, E. Dejardin, and D.R. Green. 2006. Glycogen synthase kinase-3 regulates mitochondrial outer membrane permeabilization and apoptosis by destabilization of MCL-1. *Mol. Cell*. 21:749–760. doi:10.1016/j.molcel.2006.02.009

Mavrakis, K.J., A.L. Wolfe, E. Oricchio, T. Palomero, K. de Keersmaecker, K. McJunkin, J. Zuber, T. James, A.A. Khan, C.S. Leslie, et al. 2010. Genome-wide RNA-mediated interference screen identifies miR-19 targets in Notch-induced T-cell acute lymphoblastic leukaemia. *Nat. Cell Biol.* 12:372–379. doi:10.1038/ncb2037

Mayo, L.D., and D.B. Donner. 2001. A phosphatidylinositol 3-kinase/Akt pathway promotes translocation of Mdm2 from the cytoplasm to the nucleus. *Proc. Natl. Acad. Sci. USA*. 98:11598–11603. doi:10.1073/pnas.181181198

Mu, P., Y.C. Han, D. Betel, E. Yao, M. Squatrito, P. Ogrodowski, E. de Stanchina, A. D'Andrea, C. Sander, and A. Ventura. 2009. Genetic dissection of the miR-17~92 cluster of microRNAs in Myc-induced B-cell lymphomas. *Genes Dev.* 23:2806–2811. doi:10.1101/gad.1872909

O'Hagan, R.C., N. Schreiber-Agus, K. Chen, G. David, J.A. Engelman, R. Schwab, L. Alland, C. Thomson, D.R. Ronning, J.C. Sacchettini, et al. 2000. Gene-target recognition among members of the myc superfamily and implications for oncogenesis. *Nat. Genet.* 24:113–119. doi:10.1038/72761

Olive, V., M.J. Bennett, J.C. Walker, C. Ma, I. Jiang, C. Cordon-Cardo, Q.J. Li, S.W. Lowe, G.J. Hannon, and L. He. 2009. miR-19 is a key oncogenic component of mir-17-92. *Genes Dev.* 23:2839–2849. doi:10.1101/gad.1861409

Palomero, T., W.K. Lim, D.T. Odom, M.L. Sulis, P.J. Real, A. Margolin, K.C. Barnes, J. O'Neil, D. Neuberg, A.P. Weng, et al. 2006. NOTCH1 directly regulates c-MYC and activates a feed-forward-loop transcriptional network promoting leukemic cell growth. *Proc. Natl. Acad. Sci. USA*. 103:18261–18266. doi:10.1073/pnas.0606108103

Palomero, T., M.L. Sulis, M. Cortina, P.J. Real, K. Barnes, M. Ciofani, E. Caparros, J. Buteau, K. Brown, S.L. Perkins, et al. 2007. Mutational loss of PTEN induces resistance to NOTCH1 inhibition in T-cell leukemia. *Nat. Med.* 13:1203–1210. doi:10.1038/nm1636

Payne, E.M., N. Bolli, J. Rhodes, O.I. Abdel-Wahab, R.L. Levine, C.V. Hedvat, R. Stone, A. Khanna-Gupta, H. Sun, J.P. Kanki, et al. 2011. Ddx18 is essential for cell cycle progression in zebrafish hematopoietic cells and is mutated in human acute myeloid leukemia. *Blood*. doi:10.1182/blood-2010-11-318022.

Pelengaris, S., and M. Khan. 2003. The many faces of c-MYC. *Arch. Biochem. Biophys.* 416:129–136. doi:10.1016/S0003-9861(03)00294-7

Prochownik, E.V., and P.K. Vogt. 2010. Therapeutic targeting of Myc. *Genes Cancer*. 1:650–659. doi:10.1177/1947601910377494

Radziszewska, A., D. Choi, K.T. Nguyen, S.A. Schroer, P. Tajmir, L. Wang, A. Suzuki, T.W. Mak, G.I. Evan, and M. Woo. 2009. PTEN deletion and concomitant c-Myc activation do not lead to tumor formation in pancreatic beta cells. *J. Biol. Chem.* 284:2917–2922. doi:10.1074/jbc.M805183200

Rakhra, K., P. Bachireddy, T. Zabuawala, R. Zeiser, L. Xu, A. Kopelman, A.C. Fan, Q. Yang, L. Braunstein, E. Crosby, et al. 2010. CD4(+) T cells contribute to the remodeling of the microenvironment required for sustained tumor regression upon oncogene inactivation. *Cancer Cell*. 18:485–498. doi:10.1016/j.ccr.2010.10.002

Sears, R., F. Nuckolls, E. Haura, Y. Taya, K. Tamai, and J.R. Nevins. 2000. Multiple Ras-dependent phosphorylation pathways regulate Myc protein stability. *Genes Dev.* 14:2501–2514. doi:10.1101/gad.836800

Sharma, V.M., J.A. Calvo, K.M. Draheim, L.A. Cunningham, N. Hermance, L. Beverly, V. Krishnamoorthy, M. Bhasin, A.J. Capobianco, and M.A. Kelliher. 2006. Notch1 contributes to mouse T-cell leukemia by directly inducing the expression of c-myc. *Mol. Cell. Biol.* 26:8022–8031. doi:10.1128/MCB.01091-06

Shen, W.H., A.S. Balajee, J. Wang, H. Wu, C. Eng, P.P. Pandolfi, and Y. Yin. 2007. Essential role for nuclear PTEN in maintaining chromosomal integrity. *Cell*. 128:157–170. doi:10.1016/j.cell.2006.11.042

Sodir, N.M., L.B. Swigart, A.N. Karnezis, D. Hanahan, G.I. Evan, and L. Soucek. 2011. Endogenous Myc maintains the tumor microenvironment. *Genes Dev.* 25:907–916. doi:10.1101/gad.2038411

Song, M.S., A. Carracedo, L. Salmena, S.J. Song, A. Egia, M. Malumbres, and P.P. Pandolfi. 2011. Nuclear PTEN regulates the APC-CDH1 tumor-suppressive complex in a phosphatase-independent manner. *Cell*. 144:187–199. doi:10.1016/j.cell.2010.12.020

Soucek, L., J. Whitfield, C.P. Martins, A.J. Finch, D.J. Murphy, N.M. Sodir, A.N. Karnezis, L.B. Swigart, S. Nasi, and G.I. Evan. 2008. Modelling Myc inhibition as a cancer therapy. *Nature*. 455:679–683. doi:10.1038/nature07260

Tan, Y., R.A. Timakhov, M. Rao, D.A. Altomare, J. Xu, Z. Liu, Q. Gao, S.C. Jhanwar, A. Di Cristofano, D.L. Wiest, et al. 2008. A novel recurrent chromosomal inversion implicates the homeobox gene Dlx5 in T-cell lymphomas from Lck-Akt2 transgenic mice. *Cancer Res.* 68:1296–1302. doi:10.1158/0008-5472.CAN-07-3218

Trumpp, A., Y. Refaeli, T. Oskarsson, S. Gasser, M. Murphy, G.R. Martin, and J.M. Bishop. 2001. c-Myc regulates mammalian body size by controlling cell number but not cell size. *Nature*. 414:768–773. doi:10.1038/414768a

van Riggelen, J., J. Müller, T. Otto, V. Beuger, A. Yetil, P.S. Choi, C. Kosan, T. Möröy, D.W. Felsher, and M. Eilers. 2010. The interaction between Myc and Miz1 is required to antagonize TGFbeta-dependent autocrine signaling during lymphoma formation and maintenance. *Genes Dev.* 24:1281–1294. doi:10.1101/gad.585710

Verdine, G.L., and L.D. Walensky. 2007. The challenge of drugging undruggable targets in cancer: lessons learned from targeting BCL-2 family members. *Clin. Cancer Res.* 13:7264–7270. doi:10.1158/1078-0432.CCR-07-2184

Wei, G., D. Twomey, J. Lamb, K. Schlis, J. Agarwal, R.W. Stam, J.T. Opferman, S.E. Sallan, M.L. den Boer, R. Pieters, et al. 2006. Gene expression-based chemical genomics identifies rapamycin as a modulator of MCL1 and glucocorticoid resistance. *Cancer Cell*. 10:331–342. doi:10.1016/j.ccr.2006.09.006

Weng, A.P., J.M. Millholland, Y. Yashiro-Ohtani, M.L. Arcangeli, A. Lau, C. Wai, C. Del Bianco, C.G. Rodriguez, H. Sai, J. Tobias, et al. 2006. c-Myc is an important direct target of Notch1 in T-cell acute lymphoblastic leukemia/lymphoma. *Genes Dev.* 20:2096–2109. doi:10.1101/gad.1450406

Wu, C.H., J. van Riggelen, A. Yetil, A.C. Fan, P. Bachireddy, and D.W. Felsher. 2007. Cellular senescence is an important mechanism of tumor regression upon c-Myc inactivation. *Proc. Natl. Acad. Sci. USA*. 104:13028–13033. doi:10.1073/pnas.0701953104

Wu, C.H., D. Sahoo, C. Arvanitis, N. Bradon, D.L. Dill, and D.W. Felsher. 2008. Combined analysis of murine and human microarrays and ChIP analysis reveals genes associated with the ability of MYC to maintain tumorigenesis. *PLoS Genet.* 4:e1000090. doi:10.1371/journal.pgen.1000090

Zeller, K.I., T.J. Haggerty, J.F. Barrett, Q. Guo, D.R. Wonsey, and C.V. Dang. 2001. Characterization of nucleophosmin (B23) as a Myc target by scanning chromatin immunoprecipitation. *J. Biol. Chem.* 276:48285–48291.

Zhou, B.P., Y. Liao, W. Xia, Y. Zou, B. Spohn, and M.C. Hung. 2001. HER-2/neu induces p53 ubiquitination via Akt-mediated MDM2 phosphorylation. *Nat. Cell Biol.* 3:973–982. doi:10.1038/ncb1101-973